CHEMICAL ENGINEERING TRANSACTIONS
VOL. 49, 2016
A publication of AIDIC
The Italian Association of Chemical Engineering
Online at www.aidic.it/cet
Guest Editors: Enrico Bardone, Marco Bravi, Tajalli Keshavarz
Copyright © 2016, AIDIC Servizi S.r.l.,
ISBN 978-88-95608-40-2; **ISSN** 2283-9216
DOI: 10.3303/CET1649046

Modeling Physiological Differences in Cell Populations: Acetone-Butanol-Ethanol (ABE)-Fermentation in a Cascade of Continuous Stirred Tank Reactors

Katja Karstens*[a], Sergej Trippel[a], Richard Görlitz[b], Horst Niebelschütz[b], Antonio Marzocchella[c], Peter Götz[a]

[a] Beuth University of Applied Sciences, Bioprocess Engineering, Seestrasse 64, 13347 Berlin, Germany
[b] ARGUS Umweltbiotechnologie GmbH, Kitzingstraße 11-13, 12277 Berlin, Germany
[c] Chemical Engineering Department, Università degli Studi di Napoli Federico II (UNINA), P.le V. Tecchio n. 80, Napoli, Italy
katja.karstens@beuth-hochschule.de

Acetone-Butanol-Ethanol (ABE)-fermentation with *Clostridium acetobutylicum* is a biphasic fermentation process. The formation of organic acids in the so called acidogenesis has to precede the economically interesting phase of solvent formation called solventogenesis. A separation of these metabolic phases in two or more stages of continuously run bioreactors has been successfully applied earlier (Bahl et al., 1982). However no comprehensive mathematical modeling was performed for these multi-stage processes. We now established a new experimental model system, consisting of a cascade of continuous-stirred tank reactors (CCSTR). This arrangement enables us to gain insight into metabolic phases of the ABE-fermentation with an unprecedented resolution. Experimental data collected at two dilution rates are used here to verify a mathematical model of the continuous ABE-fermentation process. This model takes into account subpopulation dynamics, meaning that a differentiation between cells with enzyme equipments adapted to acidogenic, transition and solventogenic metabolism, respectively, is made. Applying our model we found that with the differentiation from acidogenic cells to solventogenic cells takes places in the first bioreactor stage at a dilution rate of 0.042 h^{-1}, while this process is shifted to the second and third bioreactor at a dilution rate of 0.092 h^{-1}. Thus we conclude that the pH alone is not sufficient to trigger the metabolic switch between acidogenesis and solventogenesis.

1. Introduction

The production of acetone, butanol and ethanol with *Clostridium acetobutylicum* is known as ABE-fermentation. Driven by the economic interest in these solvents, intensive research on the biphasic fermentation process and its regulation has been carried out in the past decades. Most of the efforts were focused on batch processes in which the two metabolic phases, acidogenesis and solventogenesis, follow each other in time. During acidogenesis, cells take up substrate carbohydrates and convert them to organic acids (*i.e.* acetic acid and butyric acid), CO_2 and new biomass. During solventogenesis, acetic and butyric acid are taken up by the cells, which then produce butanol, acetone and ethanol. To fuel the solventogenic metabolism, carbohydrate uptake is required as well. Different mathematical models, applying various types of kinetic models, relating the switch of the metabolism to accumulating acids and/or variation of the pH, have been proposed and fitted to experimental data (*e.g.* Papoutsakis et al., 1984; Srivastava and Volesky, 1990; Liao et al., 2015). However, in batch fermentation the metabolic switch between acidogenesis and solventogenesis is overlaid by the on-set of spore formation, which makes a mathematical description challenging. The co-occurrence of solvent formation and sporulation can be avoided in continuous processes as described by Grimmler et al., 2011. Furthermore a spatial separation of the then simultaneously appearing metabolic phases can be achieved in a multi-stage continuous ABE-fermentation process (Bahl et al., 1982). However, to our knowledge no mathematical model of such a system is available so far. We therefore established a new bioreactor system, consisting of a cascade of continuous-stirred tank reactors (CCSTR).

Please cite this article as: Karstens K., Trippel S., Gorlitz R., Niebelschutz H., Marzocchella A., Goetz P., 2016, Modeling physiological differences in cell populations: acetone-butanol-ethanol (abe)-fermentation in a cascade of continuous stirred tank reactors, Chemical Engineering Transactions, 49, 271-276 DOI: 10.3303/CET1649046

This set-up enabled us to characterize different metabolic phases of the fermentation process. In parallel we set-up a computer simulation with an agent-based modeling principle that takes into account the presence of different types of cell populations in each bioreactor stage. Here we present the first application of this simulator to test a kinetic model based on three subpopulation types: acidogenic cells, intermediate cells and solventogenic cells.

2. Methods

2.1 Experimental Investigations

Continuous fermentations with *C. acetobutylicum* DSM 792 were carried out in a cascade of six linearly connected, continuous-stirred tank reactors (total volume 2.4 L) at dilution rates of 0.042 h^{-1} and 0.092 h^{-1} (*Figure 1*). The system was kept anaerobic by constant nitrogen flow. The pH in the first bioreactor tank was controlled to 4.3, while the pH in the other bioreactor tanks was kept unregulated. The continuously fed growth media contained 60 g L^{-1} glucose, 5 g L^{-1} yeast extract, 0.1 g L^{-1} KH_2PO_4, 0.2 g L^{-1} $MgSO_4$ x 7 H_20, 0.01 g L^{-1} $FeSO_4$ x 7 H_20, 0.01 g L^{-1} $MnSO_4$ x H_20 and was designed to yield phosphate limitation in the first bioreactor stage. Data were collected after establishing a steady state of the cascade, characterized by constant metabolite concentrations in the reactors. Data were collected for at least three residence times and averaged. Organic acids and solvents were quantified with GC-FID using a ZB-FFAP column (Phenomenex Inc., Torrance/USA). Glucose concentration was measured with the Reflectoquant Glucose Test (Merck KGaA, Darmstadt/Germany). Biomass concentrations were calculated by multiplying the optical density measured at a wave length of 600 nm with 0.4 g_{DM} L^{-1} OD_{600}^{-1} (Napoli et al., 2009).

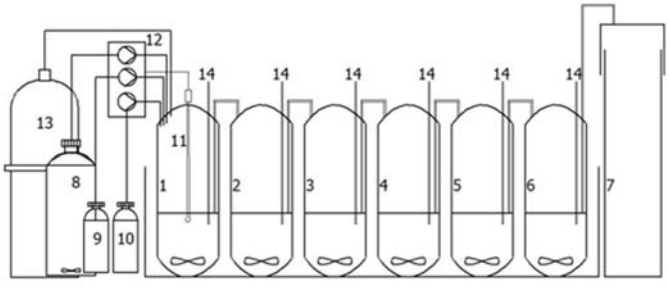

Figure 1: Cascade of continuous stirred tank reactors (CCSTR): 1-6 – CSTR; 7 – waste tank; 8 – feed tank; 9/10 – acid/base; 11 – pH electrode; 12 – control tower with pumps; 13 – Nitrogen; 14 – sampling ports

2.2 Mathematical Modelling

The agent-based model was setup with object-oriented programming (OOP) in MATLAB R2011b. The classes bioreactor_stage and subpopulation deliver blueprints for the objects (agents) of these types by defining the properties (*e.g.* position in the cascade, fill volume, dilution rate and others for bioreactor_stage) and methods (*e.g.* recalculate current concentrations or update concentrations in the influx for bioreactor_stage) that each object of this class can dispose of. Corresponding to the experimental set-up, the simulator was initialized with six bioreactor stages and three subpopulations per bioreactor stage – acidogenic, intermediate, solventogenic (*Figure 2*). However, these parameters could be adapted easily for a more detailed representation of the metabolic states. Concentrations and pH from an experimental steady state were taken as starting point. Then a simulation, consisting of an iterated calculation of the current chemical concentrations in each bioreactor stage and the biological rates of the biomass in each bioreactor, was run for a time span of 72 h with a time increment of 0.05 h. This period corresponding to at least three residence times of the cascade was enough to reach new steady state metabolite concentrations in each bioreactor. This new steady state was dependent on the kinetic model and the respective parameter set applied. Applying the kinetic model equations given in *Table 1* the correlation coefficient (1) was used as criteria to adjusted the parameter set manually to fit the experimental data recorded at D = 0.092 h^{-1}. Experimental data from steady state at D = 0.042 h^{-1} were then used for model validation. During simulation, the pH values in the bioreactor stages were kept constant on the values from the experimental data set. According to the kinetic model, subpopulation sizes were modulated by simulating growth, differentiation and transport.

correlation coefficient

$$cc = \sum_{bioreactors}^{k} \sum_{\{x;aa;ba;eth;act;but;glu\}}^{M} \left(\frac{c_{M,k}(exp) - c_{m,k}(sim)}{SD_{M,k}(exp)} \right)^2 \quad (1)$$

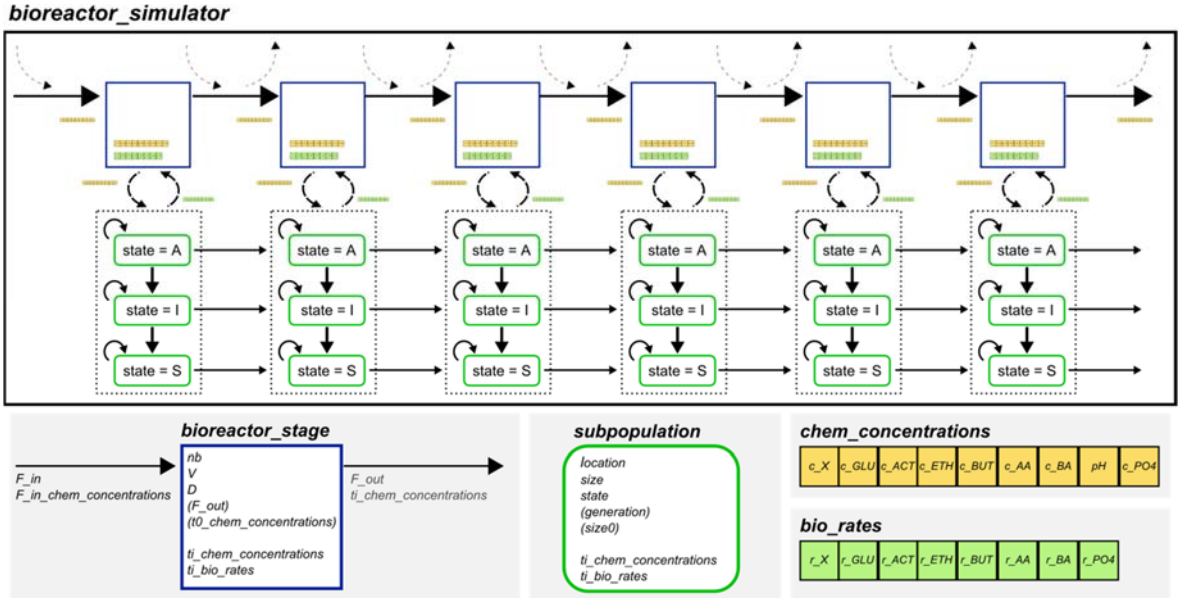

Figure 1: Architecture of the continuous, multi-stage bioreactor simulator. Chemical concentrations (8 metabolites and pH) in each bioreactor stage are changed by composition of the influx and catalytic activity of the biomass. Biomass in each reactor stage is composed of three subpopulation that show different biological rates according to their state (acidogenic (A), intermediate (I) or solventogenic (S)) and their chemical environment. Simulation includes the evolution of the biomass subpopulations, those sizes are modulated by growth, differentiation and transport.

3. Results

A newly established CCSTR was operated in steady state (*Figure 1*). This allowed us to separate the acidogenic and the solventogenic phase of the ABE-fermentation in different bioreactor tanks (*Figure 3a & 3b*). Here, we investigated two steady states corresponding to dilution rates fixed at 0.092 h^{-1} and 0.042 h^{-1}, respectively. At the higher dilution rate, equivalent to a residence time of 10.8 h, the product spectra of the first two bioreactor tanks were dominated by acetic and butyric acid, while bioreactor 5 and 6 contained predominantly butanol and acetone (*Figure 3a*). The glucose concentration decreased stepwise over the complete cascade and reached a concentration of around 5 g L^{-1} at the sixth bioreactor. At the lower dilution rate, equivalent to a residence time of 24 h, only the first bioreactor showed a product spectrum characteristic for the acidogenic phase (*Figure 3b*). In the same time solventogenic conditions were observed already in bioreactor 3. Furthermore, no changes in the product composition where observed after bioreactor 4 since glucose was depleted at this point. Thus the steady state at 0.092 h^{-1} showed a better resolution of the acidogenic-solventogenic-phase separation than at 0.042 h^{-1}, we therefore focused on this data set for the parameter fit of a newly established simulator of the CCSTR.

This simulator of the CCSTR was set up using an agent-based modeling approach. We first defined prototypes for two types of agents - bioreactor_stages and subpopulations - and equipped them with rules (kinetic laws) on how to react on different input parameters, *i.e.* concentrations of the metabolites for the subpopulation and composition of the influx and biological rates of the containing biomass subpopulations for the bioreactor stage. We then initialized the simulator with six copies of the agent type bioreactor_stage as in the experimental setup and three copies of the agent type subpopulation per bioreactor representing the acidogenic, the intermediate and the solventogenic cells, respectively (*Figure 2*). Starting from an initial data set, the system evolves towards a steady state by iterative calculations of the autonomous agents. The steady state, reached in the simulation, crucially depends on the kinetic model and the parameters applied, but not on the metabolite concentrations of the initial data set. To test the simulator we used the kinetic model given in *Table 1*, which was derived based on the works from Horvat et al. (2013) and Monot et al. (1984). Key features of this model are (I) phosphate- (and glucose-) limited growth of only solventogenic subpopulations, inhibited by increasing concentrations of butanol in a stepwise manner, (II) state-dependent organic acid formation with growth-dependent and growth-independent parts, (III) state-dependent organic acid uptake depending on the presence of the respective acid and the co-substrate glucose, (IV) state-dependent solvent formation with only growth-independent terms, (V) growth rate dependent phosphate uptake, (VI) growth rate

and product formation rates dependent glucose uptake with a state-dependent maintenance term and (VII) differentiation from acidogenic to intermediate cells and from intermediate to solventogenic cells mediated by the concentrations of undissociated organic acids. A part of the parameters used in the kinetic model was fixed to values derived from literature, Ki_{undiss} = 1.5 g L^{-1} (Monot et al., 1984), Ks_{glu} = 6.5 g L^{-1}, Ks_{AA} = 0.6 g L^{-1} and Ks_{BA} = 0.734 g L^{-1} (Srivastava and Volesky, 1990), or earlier experiments, *e.g.* $Y_{PO4/x}$ = 0.0345 g g-1 and Ki_{but} = 5 g L^{-1}. Parameters with minor influence on the simulation results, as ni_{but}, ni_{undiss} and Ks_{P04}, were approximated (see *Table 2*). Finally, cell-type-dependent parameters - μ_{max}, $r_{M\_prod\_max}$, $r_{M\_up\_max}$, $Y_{M/x}$, r_{CO2} and d_{max} - were adapted manually to fit the experimental data set recorded at D = 0.092 h^{-1}. A very good correlation between experimental and simulated steady states was achieved with the parameter set given in *Table 2* (*Figure 3a & 3c*). The correlation coefficient (1) was minimized to 41.86 for the total data set with an equal distribution of the penalty of all bioreactors (*Table 3*). For validation of the model we then applied the same parameter set for a simulation of the steady state at D = 0.042 h^{-1}. The simulation reflects the key characteristics of the experimental steady state, *i.e.* domination of the solvents starting already in the third bioreactor and depletion of the glucose in the fourth bioreactor (*Figure 3b & 3d*), while the correlation coefficient rises to 1382.18 (*Table 3*). Interestingly, the correlation between the experimental and simulated data is acceptable in the first three bioreactor stages, but declines in the later bioreactors (*Figure 3b & 3d, Table 3*). This is because of a decrease of the total biomass, observed for the third to sixth bioreactor in the experiment, which is not reproduced by the simulation as the here presented kinetic model does not include cell lysis. As consequence the butanol and acetone production and acetic and butyric acid uptake in the later bioreactors of the simulation are overestimated. Thus an adjustment of the growth model will be the next step in the iterative process of model-validation and model-extension.

Nevertheless, we got a first idea of the cell population composition in the different bioreactor stages of the cascade by the here presented simulations (*Figure 3e & 3f*) While the shift from acidogenic to solventogenic cells appears in the second and third bioreactor of the cascade run at D = 0.092 h^{-1}, the metabolic switch is already induced in the first bioreactor at D = 0.042 h^{-1}.

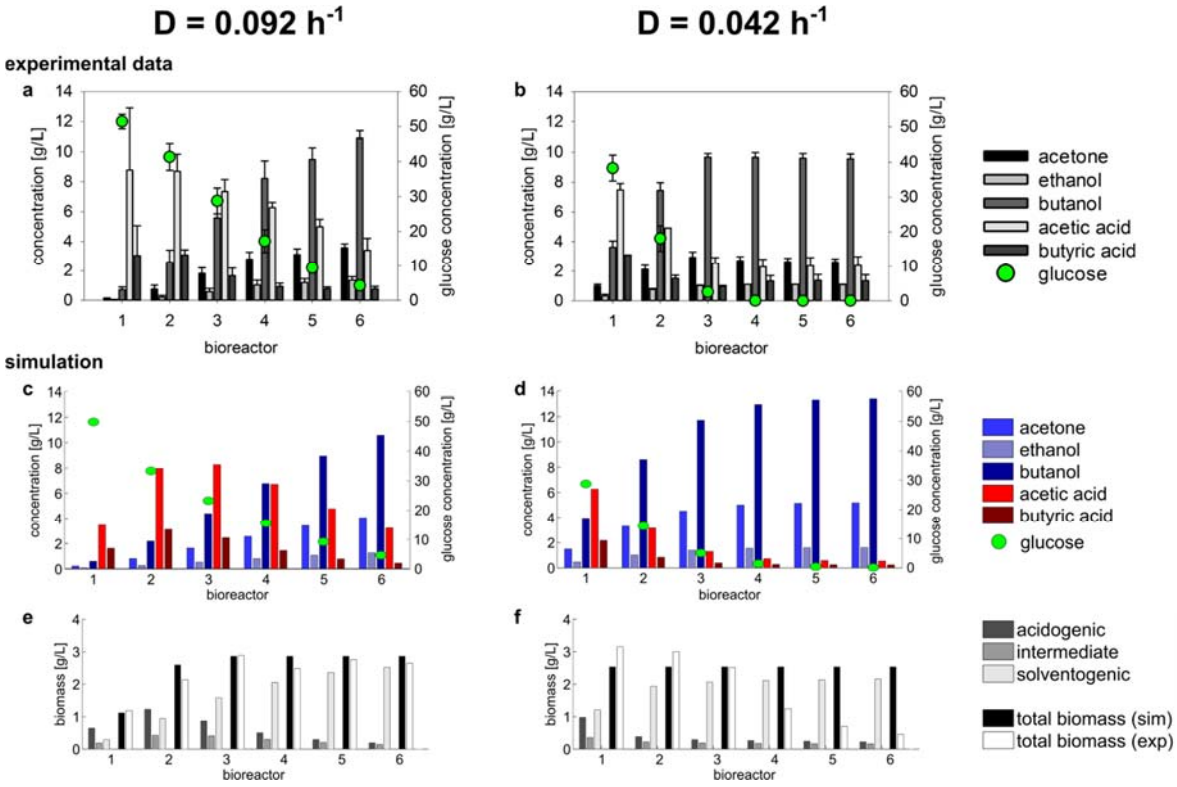

Figure 2: Comparison of metabolite concentrations in experimental (a, b) and simulated (c-f) steady states reached at dilution rates of 0.092 h^{-1} and 0.042 h^{-1}, respectively. Simulated steady states include distributions of the three subpopulations (acidogenic, intermediate and solventogenic biomass) in each bioreactor (e, f). Sums of biomasses from all subpopulations in the bioreactor are compared with the biomass concentrations found in the experiment.

Table 1: Model equations used for simulation. Highlighted parameters are state-dependent.

General balance valid for all metabolites (M) and bioreactors (k):

$$\frac{dc_{M,k}}{dt} = \frac{F_{in}}{V} \cdot c_{M,k-1} - \frac{F_{out}}{V} \cdot c_{M,k} + r_{M,k} \cdot c_{x,k} \quad (2)$$

Kinetic equations for:

biomass formation

$$r_{x,k} = \boldsymbol{\mu_{max}} \cdot \frac{c_{PO4,k}}{c_{PO4,k} + Ks_{PO4}} \cdot \frac{c_{glu,k}}{c_{glu,k} + Ks_{glu}} \cdot \frac{e^{ni_{but} \cdot (Ki_{but} - c_{but,k})}}{1 + e^{ni_{but} \cdot (Ki_{but} - c_{but,k})}} \quad (3)$$

acid and solvent production/uptake

$$r_{M,k} = r_{x,k} \cdot \boldsymbol{Y_{M/x}} + \boldsymbol{r_{M\_prod\_max}} \cdot \frac{c_{glu,k}}{c_{glu,k} + Ks_{glu}} - \boldsymbol{r_{M\_up\_max}} \cdot \frac{c_{glu,k}}{c_{glu,k} + Ks_{glu}} \cdot \frac{c_{M,k}}{c_{M,k} + Ks_M} \quad (4)$$

for M = {aa; ba; eth; act; but}

phosphate and glucose uptake

$$r_{PO4,k} = -r_{x,k} \cdot Y_{PO4/x} \quad (5)$$

$$r_{glu,k} = -(1 + \boldsymbol{r_{CO2}}) \cdot \sum_{M=\{x;aa;ba;eth;act;but\}} \left(\frac{r_{x,k} \cdot \boldsymbol{Y_{M/x}} + \boldsymbol{r_{M\_prod\_max}} \cdot \frac{c_{glu,k}}{c_{glu,k} + Ks_{glu}}}{Y_{M/glu}} \right) \quad (6)$$

biomass differentiation

$$c_{undiss} = c_{aa,k} \cdot \frac{10^{-pH}}{10^{-4.78} + 10^{-pH}} + c_{ba,k} \cdot \frac{10^{-pH}}{10^{-4.86} + 10^{-pH}} \quad (7)$$

$$d_k = \boldsymbol{d_{max}} \cdot \frac{1}{1 + e^{ni_{undiss} \cdot (Ki_{undiss} - c_{undiss,k})}} \quad (8)$$

Table 2: Parameters used for simulation. Three values are given for state-dependent parameters, corresponding to acidogenic [A], intermediate [I] and solventogenic [S] subpopulations, respectively.

metabolites (M)	$\mathbf{r_{M\_prod\_max}}$ / $\boldsymbol{\mu_{max}}$ [h^{-1}]	$\mathbf{r_{M\_up\_max}}$ [h^{-1}]	$\mathbf{Y_{M/x}}$ [g g^{-1}]	$\mathbf{Y_{M/glu}}$ [g g^{-1}]	$\mathbf{Ks_M}$ [g L^{-1}]
biomass (x)	1.16 [A] | 0.00 [I] | 0.00 [S]	-	-	0.475	-
acetic acid (aa)	1.70 [A] | 0.00 [I] | 0.00 [S]	0.00 [A] | 0.00 [I] | 1.10 [S]	1.90 [A] | 0.00 [I] | 0.00 [S]	1.136	0.600
butyric acid (ba)	1.00 [A] | 0.00 [I] | 0.00 [S]	0.00 [A] | 3.00 [I] | 0.50 [S]	1.20 [A] | 0.00 [I] | 0.00 [S]	0.833	0.734
ethanol (eth)	0.01 [A] | 0.03 [I] | 0.10 [S]	0	0	0.871	-
acetone (act)	0.00 [A] | 0.20 [I] | 0.32 [S]	0	0	0.732	-
butanol (but)	0.00 [A] | 0.70 [I] | 0.80 [S]	0	0	0.701	-
phosphate (PO4)	-	-	0.0345	-	0.005
glucose (glu)	-	-	-	-	6.500

further parameters	$\mathbf{Ki_{but}}$ [g L^{-1}]	$\mathbf{ni_{but}}$ [-]	$\mathbf{r_{CO2}}$ [h^{-1}]	$\mathbf{d_{max}}$ [h^{-1}]	$\mathbf{Ki_{undiss}}$ [g L^{-1}]	$\mathbf{ni_{undiss}}$ [-]
	5	3	0.00 [A] | 0.02 [I] | 1.20 [S]	0.40 [A] | 0.85 [I] | 0.00 [S]	1.5	3

Table 3: Correlation coefficients for simulations with the parameter set given in Table 2.

	total	**bioreactor 1**	**bioreactor 2**	**bioreactor 3**	**bioreactor 4**	**bioreactor 5**	**bioreactor 6**
0.092 h^{-1}	41.86	3.59	10.12	7.69	11.05	1.69	7.72
0.042 h^{-1}	1382.18	52.96	116.31	163.99	255.29	378.21	415.42

4. Discussion

We here present the first application of a new agent-based model for simulation of ABE-fermentation processes in a CCSTR. This type of model offers the advantage to be easily extendable to multiple bioreactor stages and biomass subpopulations and easily adaptable to new kinetic models. However no effective parameter estimation algorithm is available at this point. Establishing an automated parameter estimation with a reasonable calculation demand will thus be the focus of our future research. Nevertheless, even in the present state the simulator allowed the evaluation of a here proposed kinetic model based on the presence of three types of cells characterized by acidogenic metabolism, by metabolism of the transition phase or by solventogenic metabolism. The here presented simulations deliver insight in the possible composition of the biomass in each bioreactor tank. Our model implies that the metabolic switch is already induced in the first bioreactor at D = 0.042 h^{-1}, while the first bioreactor of the cascade run at D = 0.092 h^{-1} is dominated by acidogenic cells, though both bioreactor stages are regulated at pH 4.3. This leads to the hypothesis that the pH alone is not sufficient to trigger the switch from acidogenesis to solventogenesis as assumed in earlier models (Millat et al., 2013). To clarify the regulatory mechanisms behind the switch of clostridial metabolism, the consideration of intracellular fluxes might be important. Due to the flexibility of the simulator we will also be able to test structured kinetic models taking into account selected intracellular metabolites as in the works of Liao et al. (2015) and Millat et al. (2013) in future studies. Furthermore, the simulator allows us to analyse the impact of additional feeding points as in Horvat et al. (2013) and recirculation between bioreactor stages. Once validated such models will enable us to determine optimal feeding and pH control strategies for a continuous butanol production process.

5. Conclusions

This work presents the first step of an agent-based model for a continuous, multi-stage ABE-fermentation process. The here described simulator takes into account the presence of different types of subpopulation in each bioreactor tank, characterized by different catabolic activities. It further enables the conversion of cells from one subpopulation type to another and thus forms the fundament for testing different hypotheses of what triggers such metabolic switches.

Acknowledgments

This work is part of the OPTISOLV project, supported within the frame of the ERA-Net EuroTransBio-7 initiative by the German Federal Ministry of Education and Research under reference number 031A231C.

Reference

Bahl H., Andersch, W. and Gottschalk G., 1982, Continuous Production of Acetone and Butanol by Clostridium acetobutylicum in a Two-Stage Phosphate Limited Chemostat, European J Appl Microbiol Biotechnol, 15, 201-205.

Grimmler C., Janssen H., Krausse D., Fischer R. J., Bahl H., Dürre P., Liebl W., Ehrenreich A., 2011, Genome-wide gene expression analysis of the switch between acidogenesis and solventogenesis in continuous cultures of Clostridium acetobutylicum, J Mol Microbiol Biotechnol, 20, 1-15.

Horvat P., Spoljarric I.V., Lopar M., Atlic A., Koller M., Braunegg G., 2013, Mathematical modelling and process optimization of a continuous 5-stage bioreactor cascade for production of poly[-(*R*)-3-hydroxybutyrate] by *Cupriavidus necator*, Bioprocess Biosyst Eng, 36, 1235-1250.

Liao c., Seo s., Celik V.,Lui H., Kong W., Wang Y. Blaschek H., Jin Y.-S., Lu T., 2015, Integrated, systems metabolic picture of acetone-butanol-ethanol fermentation by *Clostridium acetobutylicum,* Proc Natl Acad Sci USA, 112,201423143.

Millat T., Janssen H., Thorn G., King J., Bahl H., Fischer R., Wolkenhauer O., 2013, A shift in the dominant phenotype governs the pH-induced metabolic switch of *Clostridium acetobutylicum* in phosphate-limited continuous cultures, Appl Microbiol Biotechnol, 97, 6451-6466.

Monot F., Engasser J.-M., Petitdemange H., 1984, Influence of pH and undissociated butyric acid on the production of acetone and butanol in batch cultures of *Clostridium acetobutylicum*, Appl Microbiol Biotechnol, 19, 422-426.

Napoli F, Olivieri G, Marzocchella A, Salatino P, 2009, An assessment of the kinetics of butanol production by *Clostridium acetobutylicum* Int J Chem Reactor Eng, 7:A45

Papoutsakis E. T., 1984, Equations and calculations for fermentations of butyric acid bacteria, Biotechnology and Bioengineering, 26, 174-187.

Srivastava A., Volesky B., 1990, Updated model of the batch acetone-butanol fermentation, Biotechnology letters, 12, 693-698.